Operating characteristics of nebulizers used for intraperitoneal aerosolized drug delivery

Mohammad Rahimi-Gorji[1,2,3#*], Lotte Desmet[2#], Stéphane Dorbolo[4], Charlotte Debbaut[2,3], Sarah Cosyns[1,3], Wouter Willaert[1,3], Wim Ceelen[1,3*]

[1]Laboratory of Experimental Surgery (SURGX), Department of Human Structure and Repair, Ghent University, Ghent 9000, Belgium

[2]IBiTech-BioMMedA, Department of Electronics and Information Systems, Ghent University, Ghent 9000, Belgium

[3]Cancer Research Institute Ghent, Corneel Heymanslaan 10, Ghent 9000, Belgium

[4]PtYX, Soft Matter Pole, CESAM, Université de Liège, Liège 4000, Belgium

[#] Equal contributions

[*] Corresponding authors

Abstract

Intraperitoneal aerosolized drug delivery (IPADD) is a minimally invasive technique for treating peritoneal metastasis (PM), combining diagnostic laparoscopy with locoregional chemotherapy delivery as an aerosol. This study investigates key operational and physiological factors affecting IPADD outcomes, focusing on aerosolization pressure, droplet size distribution (DSD), and spray cone angle using six nebulizers (Capnopen, Capnopharm, HurriChem, MCR-4 TOPOL, QuattroJet, and MiniJet) in a reconstructed peritoneal cavity model. Results indicate notable variations in nebulizer performance. Capnopen, Capnopharm, and HurriChem showed similar technical characteristics and reliable performance. DSD analysis revealed bimodal distributions, with MiniJet and HurriChem producing finer droplets (10–20 µm), while MCR-4 TOPOL generated coarser droplets due its larger orifice and distinctive design. Spray cone angle measurements demonstrated that higher flow rates slightly improved dispersion, with the MCR-4 TOPOL achieving the widest angles. Optimal flow rates for uniform spray patterns varied, with Capnopharm and HurriChem performing well at lower rates, while MCR-4 TOPOL and QuattroJet required higher flow rates (>1.0 mL/s). This comprehensive evaluation provides valuable insights to optimize nebulizer selection and aerosolized drug delivery for improved IPADD efficacy.

Keywords: Intraperitoneal aerosolized drug delivery (IPADD); Operational pressure; Droplet size distribution; Spray cone angle.

Introduction

Intraperitoneal aerosolized drug delivery (IPADD)

Peritoneal metastasis (PM) refers to the spread of malignant cells within the peritoneal cavity, and it is associated with a significantly poorer prognosis compared to metastases at other sites. This is largely due to the limited penetration of anticancer drugs in the peritoneal tissues, which restricts their effectiveness (Kobayashi & Kodera, 2017; Nadiradze et al., 2019). Traditional chemotherapy poses challenges in treating PM effectively, as systemic administration often leads to suboptimal drug delivery to the peritoneal surface and increases systemic toxicity. To address this, intraperitoneal (IP)

chemotherapy has emerged as a promising alternative, aiming to enhance localized drug uptake while reducing systemic exposure (Alyami et al., 2019). However, high intraperitoneal drug concentrations do not always translate to improved tissue penetration, and drug distribution remains uneven, leaving poorly treated or untreated regions within the peritoneum (Ceelen, Braet, Van Ramshorst, Willaert, & Remaut, 2020; Khosrawipour et al., 2016; Nadiradze et al., 2019).

Intraperitoneal aerosolized drug delivery (IPADD, also known as 'pressurized intraperitoneal aerosol chemotherapy' or PIPAC) has been developed as a minimally invasive technique to improve drug delivery specifically for PM. This approach aerosolizes chemotherapy drugs within the peritoneal cavity, utilizing aerosolized droplets to achieve closer contact with the disease site, potentially increasing efficacy while minimizing systemic side effects. During IPADD, CO_2 gas is used to insufflate the peritoneal cavity to a pressure of 12–15 mmHg. The chemotherapy drug is then aerosolized under pressure using a high-pressure pump (Injektron 82 M, Medtron AG, Saarbrücken, Germany) and nebulizer, which disperses the droplets across the peritoneal surface and targets cancer cells more effectively (see Fig. 1). The aerosolized chemotherapy remains in the cavity for 30 minutes, enhancing its interaction with the peritoneal surface.

Physical parameters, including droplet size, density, forces acting on the droplets, aerosol viscosity, and even the application of an electrostatic field, have been shown to influence the spatial distribution of the aerosol and thus its uptake by peritoneal tissues (Rahimi-Gorji et al., 2022; Rahimi-Gorji, Ghorbaniasl, Cosyns, Willaert, & Ceelen, 2021). However, certain physiological factors that may further impact the effectiveness of IPADD have not been fully explored. This study focuses on quantifying critical parameters such as aerosol pressure, droplet size distribution within a closed cavity, and additional physiological factors like relative humidity (RH), temperature (T), and pH. By investigating these factors, we aim to deepen the understanding of IPADD dynamics and identify ways to optimize its therapeutic outcomes.

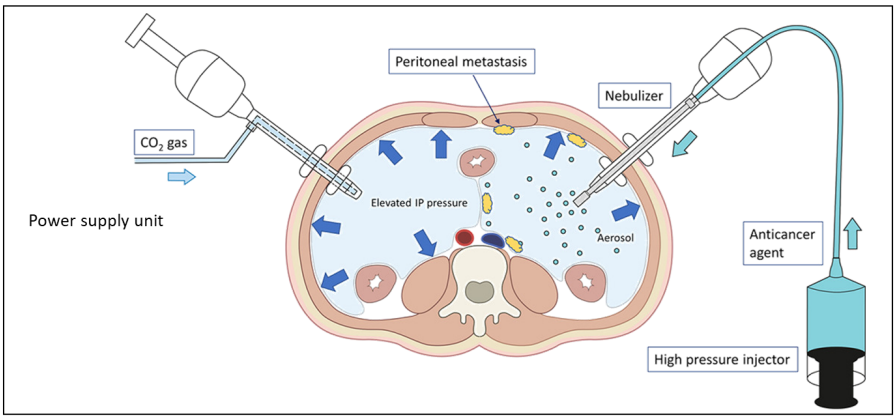

Fig. 1. Schematic illustration of intraperitoneal aerosolized drug delivery (IPADD) (Rahimi-Gorji et al., 2020)

Aerosolization

An aerosol is defined as a suspension of fine solid particles or liquid droplets within a carrier fluid, either liquid or gas (Meyers, 1992). Naturally occurring aerosols include fog and mist, while

anthropogenic aerosols include smoke and air pollutants. The medical application of aerosols has a rich history, evolving from ancient inhalation practices using aromatic plant leaves to today's advanced aerosolized drug delivery systems in pulmonary and intraperitoneal medicine (Stein & Thiel, 2017). Aerosolized drug delivery enables precise, localized administration, particularly valuable for treating conditions within closed cavities, such as the peritoneal cavity, by creating an aerosolized mist of therapeutic agents that directly targets affected areas.

In IPADD, medications are nebulized directly into the peritoneal cavity, allowing for enhanced tissue exposure. This technique offers notable advantages, including direct delivery to the peritoneal cavity for rapid drug absorption by abdominal organs, which may enhance therapeutic effects. Concentrating the drug within the peritoneum reduces systemic exposure, often allowing for lower doses and minimizing systemic side effects. It also supports post-operative management by alleviating pain and inflammation. However, this method presents challenges, such as achieving precise control over drug dosing and distribution within the cavity, which is crucial for effective treatment. There are occupational safety risks, including unintentional inhalation of aerosolized particles, necessitating strict protective protocols. Additionally, as with any intraperitoneal procedure, there is a risk of infection.

In the IPADD technique, until 2022, only a specialized pressure-swirl nebulizer was used to aerosolize the drug within the peritoneal cavity. The original nozzle which was used for off-label IPADD is a CE certified class IIa device to aerosolize aqueous drug solutions. This nebulizer is a critical component, designed as a pressure-swirl atomizer that is commonly applied in fields such as fuel injection, spray coating, and aerosol generation. The pressure-swirl atomizer transforms a high-pressure liquid stream into a fine mist through the swirling motion of the liquid within a spin chamber. Within the nebulizer, the liquid undergoes intense swirling, creating a central air core that stabilizes and enhances the swirling action. The swirling action causes the liquid to exit as a thin film, where natural instabilities lead to film breakup into ligaments. These ligaments either fragment further or contract into spherical droplets under surface tension forces, completing the primary atomization process. This mechanism ensures that the aerosol droplets are small, uniform, and capable of widespread peritoneal distribution, maximizing surface contact with peritoneal tissues.

Recently, new nebulizer devices are also in clinical use. While the technical and clinical performance data of the original IPADD nozzle has been extensively studied in pre- and clinical settings (Göhler, Khosrawipour, et al., 2017; Sgarbura et al., 2021), very limited comparative data are available for the new IPADD nozzles (Göhler, Oelschlägel, Ouaissi, & Giger-Pabst, 2024). Oncological surgeons around the world are now faced with the question of whether these newer nozzles are equivalent to the original nozzle technology or perhaps even have technical/functional advantages with a potentially better oncological outcome.

Until 2022, the IPADD technique relied exclusively on a specialized pressure-swirl nebulizer to aerosolize drugs within the peritoneal cavity. This original nozzle, a CE-certified Class IIa device, was designed to aerosolize aqueous drug solutions and has roots in applications like fuel injection and spray coating. It works by generating a high-pressure swirl that transforms the liquid into a fine mist, creating small, uniform droplets ideal for wide peritoneal distribution and optimal tissue contact.

The nebulizer produces a polydisperse, bimodal aerosol with a volume-weighted median droplet diameter of 25-30 µm, covering a spray cone of approximately 70°. Recently, new nebulizers have entered clinical use, yet comprehensive comparative data on their efficacy versus the original IPADD nozzle remains limited (Göhler, Khosrawipour, et al., 2017; Göhler et al., 2024; Sgarbura et al., 2021). This raises important questions for oncological surgeons regarding whether these new nozzles match or potentially surpass the original in technical performance and therapeutic outcomes.

This research aims to build on existing knowledge by examining critical parameters such as aerosol pressure, droplet size distribution, and environmental factors like relative humidity, temperature, and pH within the closed cavity. By refining these variables, we aim to improve the delivery efficiency and therapeutic impact of intraperitoneal aerosolized drug administration.

Commenté [MOU1]: could be in the perspectives

Materials and methods

All experiments were performed in the Laboratory of Experimental Surgery (SurgX, Department of Human Structure and Repair, Ghent University Hospital, Ghent , Belgium) and Laboratory of Pharmaceutical Technology (Faculty of Pharmaceutical Sciences, Ghent University, Ghent, Belgium) at a room temperature *T* equal to 20-21 °C. Six single-substance IPADD nebulizers for intraperitoneal aerosolized drug delivery were examined, i.e., Capnopen (REGER 770–12) (REGER Medizintechnik, Villingendorf, Germany), Capnopharm (CapnoPharm GmbH, Tübingen, Germany), HurriChem™ (ThermaSolutions, White Bear Lake, MN, USA), MCR-4 TOPOL (SKALA-Medica, Soběslav, Czech Republic), QuattroJet (REGER 770–14), and MiniJet (REGER 770-15) (REGER Medizintechnik, Villingendorf, Germany).

a supprimé: of T=

a mis en forme : Police :Italique

Measurement of operational pressure

Based on the upstream pressure, the liquid solution can be nebulized considering the expected flow rate. To characterize operational pressure relative to volumetric flow rate, the nebulizers were connected via a high-pressure line to a high-pressure pump (Accutron CT roller, MEDTRON AG, Saarbruecken, Germany) to deliver a saline solution (0.9% NaCl) through the nebulizers. A pressure transmitter (Turck PT300PSIG-1003-U1-H1143, Turck Inc., Minnesota, USA) which was connected to a DC power modules (TMT Series, TracoPower, 6340 Baar Switzerland) using an actuator and sensor cable (model RKC4.4T-2/TXL, Hans Turck GmbH & Co. KG) was used to measure operational pressure induced by varying liquid flow rates. This sensor was calibrated using a secondary pressure sensor (Dwyer, Michigan City, USA), with calibration achieved by applying linear regression to the measured data, resulting in the following linear relationship between the known pressure (P_{true}, from the Dwyer sensor) and the measured pressure (P_{op}, from the Turck sensor):

Commenté [MOU2]: A better name than 'true' ?

$$P_{true} = 1.1794\, P_{op} + 0.025 \qquad (1)$$

The operational pressure was examined at three different volumetric flow rates (0.5, 0.8, and 1.1 mL/s) until the maximum pressure of 21 bar for the high-pressure pump was reached. For the Quattrojet nebulizer, a flow rate of 1.5 mL/s was also tested. Data acquisition was conducted using a PowerLab 8/35 datalogger (ADInstruments, Sydney, Australia) connected to a PC running LabChart software.

To compare the pressure of the saline solution as it exited the syringe and as it reached the nebulizer, two distinct setups were utilized (see Fig. 2). In the first setup as configuration 1, the pressure sensor and nebulizer were positioned directly after the syringe on the pump. In the second setup as configuration 2, a high-pressure tube was connected to the syringe, with the pressure sensor and nebulizer placed downstream of this tube, aligned at the same height. At these two target positions, a 3-way Y-shaped manifold (FLL, FLL, MLL, Cadence Science, Inc., Cranston, RI, USA) was implemented. For each nebulizer type, pressure was measured in both configurations. All experiments were conducted under steady-state aerosolization conditions and repeated in triplicate to ensure reproducibility.

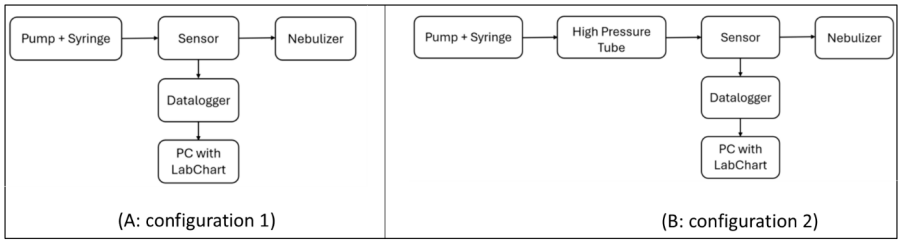

Fig. 2. Experimental setup configurations for comparing operational pressure during IPADD. In Configuration 1, the pressure sensor and nebulizer were positioned directly after the syringe on the pump. In Configuration 2, a high-pressure tube was connected to the syringe, with the pressure sensor and nebulizer placed downstream of the tube, aligned at the same height.

Measurement of droplet size distribution

The size of aerosol droplets plays a critical role in the forces acting upon them, directly influencing the spatial distribution of the aerosol. The droplet size is also a crucial parameter regarding the result of its impact on the surface (see for example Rioboo2001, Parmentier2023). As droplet size increases, both drag force and, more notably, gravitational force become increasingly significant in governing aerosol transport (Rahimi-Gorji et al., 2022). Consequently, investigating the droplet size distribution (DSD) during IPADD is essential for a deeper understanding of this process.

a supprimé: R. Rioboo, C. Tropea, and M. Marengo, Outomes from a drop impact on solid surfaces, Atomization and Sprays 11 (2001) 155 or (more local and recent)

a supprimé: , J. Parmentier, V. Terrapon, and T. Gilet, Physical Review Fluids 8 (2023) 053603

For this experiment, the same high-pressure pump (Accutron CT roller, MEDTRON AG) was used, and the nebulized fluid was saline (NaCl 0.9%). Measurements of the volume weighted DSD of aerosol droplets was performed experimentally using laser diffraction (Mastersizer S long bench, Malvern Instruments, Malvern, United Kingdom). An open laser beam (water vs. air, refractive index of 1.33 and 1.00, respectively) was created with a 300F lens (0.5–900 µm) after 10 s of nebulization. When the aerosol droplets interfere with the laser beam, they create a diffraction pattern. The laser diffraction instrument allows obtaining the size distribution of aerosol droplets by measuring the angular variation in intensity of light scattered as a laser beam passes through the droplets.

Measurements were conducted in a closed cavity modeled after a realistic, patient-based peritoneum geometry (see Fig. 3a). The 3D peritoneal cavity model was positioned at an optimal height within the Mastersizer S, allowing the laser to pass through designated optical windows on either side of the model. Nebulizers were inserted at the top of the model. Before starting the experiment, the laser was carefully aligned. Droplet size distribution was measured at distances of 5 cm and 15 cm from the nebulizer tip and the lens, respectively. Nebulization was then initiated at the specified flow rate with a set volume of 40 mL. Measurements began once the nebulization stabilized, reaching full intensity after approximately 10 seconds. At this point, the device started analyzing the droplet size distribution. After each measurement, the nebulization process was stopped. For each nebulizer, droplet size distribution was recorded at flow rates of 0.5, 0.8, and 1.1 mL/s. For the QuattroJet, a flow rate of 0.5 mL/s was not tested; instead, a flow rate of 1.5 mL/s was used. Each experiment was conducted in triplicate.

Results were exported as the median of the volume distribution, D(v,0.5), i.e. the volume median diameter at which 50 vol% of the aerosol droplets were either finer or coarser than the predicted value, with standard deviation.

Fig. 3b, shows the setup for measuring volume-weighted droplet size distribution in the closed cavity.

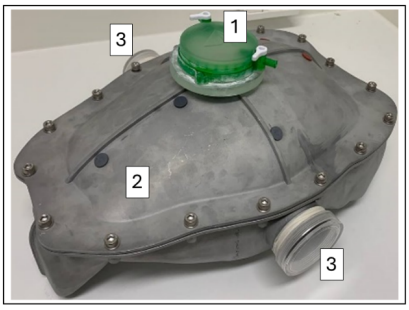

(a)

1. Gel-port for inlet (nebulizer)
2. Reconstructed peritoneal cavity
3. Optical windows
4. Laser distraction instrument
5. Nebulizer

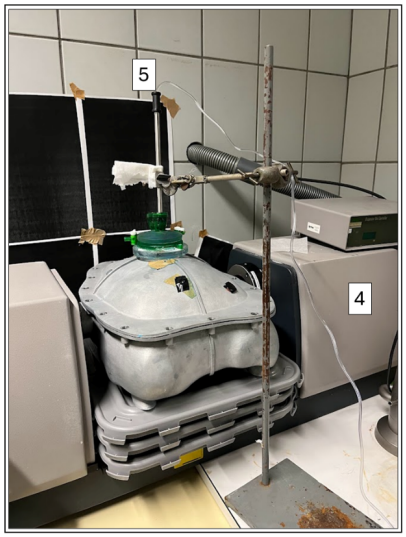

(b)

Fig. 3. (a) The manufactured aluminum model of the peritoneal cavity using a realistic, patient-based model, and (b) setup for measuring volume-weighted droplet size distribution in the closed cavity.

Measurement of orifice size and spray cone angle

The nozzle geometry and characteristics affect the aerosol droplet behavior during nebulization. The diameter of the orifice and the cone angle of nebulization are two given characteristics of the nozzle by the manufacturer. The cone angle has a relationship with the driving pressure, flow rate, and viscosity of the fluid. Fig. 4 shows the experimental setup of high-speed imaging used to measure the cone angle of nebulization. The experiments were performed using saline (0.9% NaCl) and flow rates of 0.8 and 1.1 mL/s with a maximal pressure of 21 bar.

During each experiment, digital images were obtained using a high-speed camera (3200 frames/second- Phantom MIRO M310, Adept Turnkey Pty Ltd, Western Australia) during nebulization. The camera was fixed on a tripod and was positioned perpendicular direction and 20 cm far from to the tip of nebulizer. One plane photographic image was captured at a resolution of 512 pixels (corresponding to 9.22 µm/pixel). The high-speed images were analyzed using ImageJ software (version 1.51, National Institutes of Health, Bethesda, Maryland, United States). The cone angle was determined by defining two edges drawn in a plane from the nozzle tip to the outer periphery of the aerosol. The recorded time for each experiment was set to 1 s. Time step between every two images was set at 100 µs.

Description of the different used nozzles in the study.

Fig. 7 provides a microscopic view of the orifices of the various nebulizers used in this study. High-speed camera imagery (Phantom) was employed to capture detailed photographs, ensuring precise measurements of the orifice diameters. Calibration of the scale was conducted using a known

a supprimé: Fig. 7 provides a microscopic view of the orifices of the various nebulizers used in this study. High-speed camera imagery (Phantom) was employed to capture detailed photographs, ensuring precise measurements of the orifice diameters. Calibration of the scale was conducted using a known reference, enabling accurate pixel-to-distance conversion. The measured diameters of the nebulizer orifices were as follows: Capnopen: Ø ≈ 190 ± 2 µm; Capnopharm: Ø ≈ 186 ± 4 µm; HurriChem: Ø ≈ 191 ± 2 µm; MCR-4 TOPOL: Ø ≈ 389± 6 µm; QuattroJet : Ø ≈ 190 ± 2 µm; MiniJet: Ø≈160±2 µm. These measurements demonstrate significant variations in orifice sizes, which are expected to influence the spray characteristics.

a supprimé: tripod, and

a supprimé: images

Commenté [MOU3]: The number of the figures should be changed if we adopt this way of presenting the nozzle before the experimental results

reference, enabling accurate pixel-to-distance conversion. The measured diameters of the nebulizer orifices were as follows: Capnopen: Ø ≈ 190 ± 2 µm; Capnopharm: Ø ≈ 186 ± 4 µm; HurriChem: Ø ≈ 191 ± 2 µm; MCR-4 TOPOL: Ø ≈ 389± 6 µm; QuattroJet : Ø ≈ 190 ± 2 µm; MiniJet: Ø≈160±2 µm. These measurements demonstrate significant variations in orifice sizes, which are expected to influence the spray characteristics.

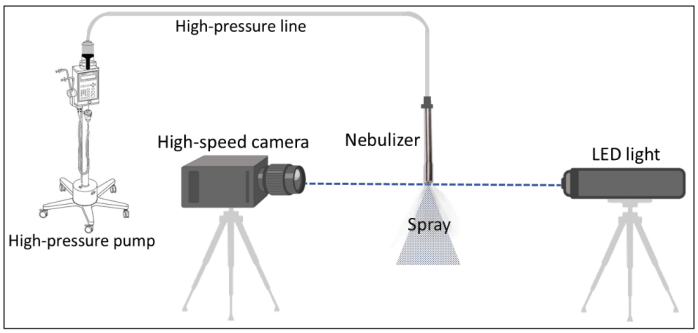

Fig. 4. Schematic illustration of high-speed imaging to visualize the cone angle of spray.

Results

Measured practical pressure during IPADD

Fig. 5 provides a comparative analysis of median operational pressures over time for two different configurations, measured across various nebulizers at three distinct flow rates (0.5, 0.8, and 1.1 mL/s). The shaded regions represent the standard deviations, capturing the variability in pressure for each configuration.

The data reveals distinct maximum pressures for each nebulizer, highlighting significant differences in their mechanical and operational capacities. These pressure variations can impact tissue penetration (with higher pressures enabling deeper penetration), droplet size and consistency, and the aerosol's spatial distribution, affecting coverage uniformity

The pressure data were fitted using a phenomenological sigmoid function:

$$P = \frac{\Delta P}{1+e^{-k(t-t_0)}} + b \qquad (2)$$

where the term b represents the vertical shift, setting the baseline level, ΔP represents the asymptotical pressure variation starting from the baseline b. The parameter k determines the growth rate and steepness of the curve, while t_0 corresponds to the inflection point time, namely when $P = \Delta P/2$. This approach allows the extrapolation of the maximum pressure at infinite time, $P_{max}=\Delta P-b$. In Fig. 5, the black dashed lines represent the fitted curves overlaid on the original pressure data.

Table 1 summarizes the maximum median operational pressure, the time required to reach this pressure, and the extrapolated maximum pressure at infinite time for two configurations (1 and 2) and three flow rates (0.5, 0.8, and 1.1 mL/s) across six nebulizers.

Table 2 presents the curve-fitting parameters for the extrapolated function applied to the operational pressure values for configurations 1 and 2.

Commenté [MOU4]: I would put the measurement of size hole here before the experiments. This allows to have an idea on the different nebulizer geometries. For the Fig. 7, it could be better to put only the holes on the same scale. The diameters are nearly the same for all the nebulizer (190µm) and the distribution of the droplets is always bimodal.

a supprimé: I would put the measurement of size hole here before the experiments. This allows to have an idea on the different nebulizer geometries. For the Fig. 7, it could be better to put only the the holes on the same scale. The diameters are nearly the same for all the nebulizer (190µm) and the distribution of the droplets is always bimodal. ¶

a déplacé vers le bas [1]: Among the nebulizers tested, the Capnopen nebulizer consistently achieved the highest pressures across all flow rates, peaking immediately at the start of nebulization, particularly at a flow rate of 1.1 mL/s, where the pressure reached 21 bar almost immediately. This rapid rise suggests that the Capnopen is particularly well-suited for low flow rate applications.¶
nebulizer demonstrated the second-highest pressures, followed closely by the MCR-4 Topol. These nebulizers displayed a steady increase in pressure but did not reach the same peak as the Capnopen . Conversely, the Quattrojet exhibited the lowest operational pressures, suggesting it may be better suited for high flow rate applications.¶

a supprimé: *y*

a supprimé: *L*

a supprimé: *x*

a supprimé: *x*

a supprimé: *L*

a supprimé: maximum asymptote

a supprimé: , defining the upper bound of growth

a supprimé: *x*

a supprimé: re

a supprimé: *y*

a supprimé: *L*

a supprimé: The term *b* represents the vertical shift, setting the baseline level.¶

a mis en forme : Police :Italique

Commenté [MOU5]: I do not think that it is necessary to give the value of all the parameters since only the max pressure matters

Among the nebulizers tested, the Capnopen nebulizer consistently achieved the highest pressures across all flow rates, peaking immediately at the start of nebulization, particularly at a flow rate of 1.1 mL/s, where the pressure reached 21 bar almost immediately. This rapid rise suggests that the Capnopen is particularly well-suited for low flow rate applications.

The Capnopharm nebulizer demonstrated the second-highest pressures, followed closely by the MCR-4 Topol. These nebulizers displayed a steady increase in pressure but did not reach the same peak as the Capnopen. Conversely, the Quattrojet exhibited the lowest operational pressures, suggesting it may be better suited for high flow rate applications.

Note that for some nebulizer nozzles and at high flow rate, the saturation of the pressure was not reached. That means that we do not reach a steady state for the generation of the droplets. This problem occurs for Capnopen, capnopharm, Hurrichem, Minijet and MCR-4. Quattrojet allows to reach a steady pressure after 30 s in all the envisaged cases.

a déplacé (et inséré) [1]

Configuration 1	Configuration 2
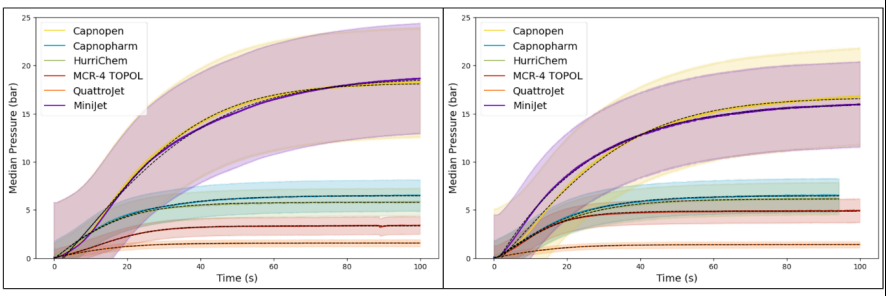	
(a) Flow rate= 0.5 mL/s	
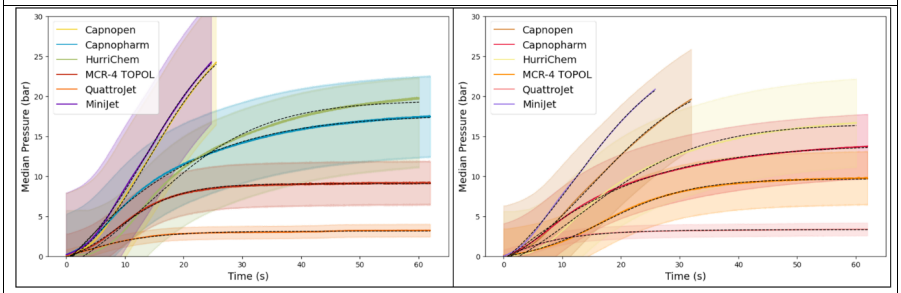	
(b) Flow rate= 0.8 mL/s	

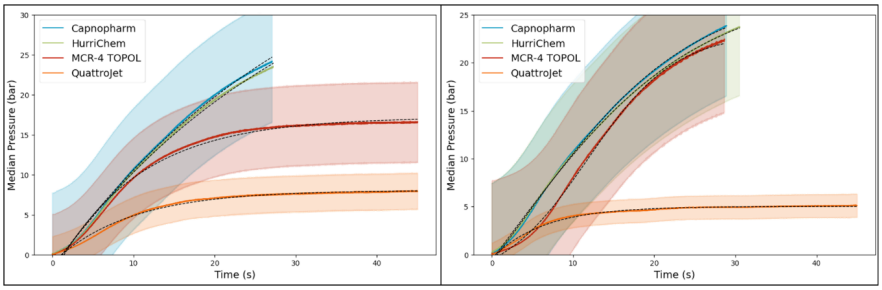

(c) Flow rate= 1.1 mL/s

Fig. 5. Median operational pressure over time for two configurations (1 and 2) and three flow rates (0.5, 0.8, and 1.1 mL/s) across different nebulizers. For the Capnopen and MiniJet nebulizers at flow rate of 1.1 mL/s, the maximum pressure was reached immediately upon the start of nebulization. The black dashed lines represent the fitted curves overlaid on the original pressure data.

Table 1. The maximum median operational pressure, the time required to reach this pressure, and the extrapolated maximum pressure at infinite time for two configurations (1 and 2) and three flow rates (0.5, 0.8, and 1.1 mL/s) across six nebulizers. For the Capnopen nebulizer at flow rate of 1.1 mL/s, the maximum pressure was reached immediately at the start of nebulization.

Nebulizer	Flow rate (mL/s)	Configuration 1			Configuration 2		
		Avg. max. pressure (bar)	Extrapolated max. pressure (bar)	Time (sec)	Avg. max. pressure (bar)	Extrapolated max. pressure (bar)	Time (sec)
Capnopen	0.5	15.56	18.18	99.92	14.31	16.71	99.52
	0.8	21.18	28.29	26.54	21.18	27.62	34.54
	1.1	-	-	-	-	-	-
Capnopharm	0.5	5.92	6.48	92.72	5.92	6.45	92.72
	0.8	14.93	17.73	61.81	13.8	16.62	61.88
	1.1	21.18	27.56	28.82	20.79	27.58	30.71
HurriChem	0.5	5.80	5.77	96.65	5.36	6.14	96.67
	0.8	16.64	19.47	65.29	15.84	19.47	64.47
	1.1	20.55	27.65	28.82	20.17	27.68	30.71
MCR-4 TOPOL	0.5	2.94	3.34	96.82	4.33	4.86	96.93
	0.8	7.88	9.05	58.49	9.87	11.34	62.04
	1.1	14.13	16.42	43.31	20.38	23.10	35.49
QuattroJet	0.5	1.36	1.55	71.45	1.22	1.39	81.63
	0.8	2.78	3.13	57.01	3.47	3.91	54.80
	1.1	6.81	7.77	44.39	4.39	5.02	45.49

MiniJet	0.5	15.87	18.75	101.06	13.58	16.14	99.52
	0.8	21.18	29.66	28.31	21.18	30.35	26.33
	1.1	-	-	-	-	-	-

Table 2. Parameters of the curve-fitting extrapolated function $P = \frac{\Delta P}{1+e^{-k(t-t_0)}} + b$ *for the operational pressure values for two configurations (1 and 2) and three flow rates (0.5, 0.8, and 1.1 mL/s), evaluated for six nebulizers.*

Nebulizer	Flow rate (mL/s)	Parameters							
		Configuration 1				Configuration 2			
		ΔP	t_0	k	b	ΔP	t_0	k	b
Capnopen	0.5	27.79	12.35	0.06	-9.60	30.20	5.90	0.06	-13.49
	0.8	32.74	14.43	0.15	-3.75	33.16	15.16	0.12	-5.54
	1.1	-	-	-	-	-	-	-	-
Capnopharm	0.5	28.44	-17.68	0.07	-21.96	13.19	0.07	0.08	-6.74
	0.8	52.54	-8.85	0.07	-34.81	55.38	-12.77	0.06	-38.75
	1.1	39.58	7.77	0.12	-12.02	47.67	3.96	0.10	-20.09
HurriChem	0.5	12.33	-1.18	0.09	-6.56	12.53	0.06	0.08	-6.40
	0.8	25.90	13.85	0.10	-6.42	25.93	13.85	0.10	-6.46
	1.1	4.47	1.39	3.13	-1.69	52.55	1.73	0.09	-24.86
MCR-4 TOPOL	0.5	4.18	11.41	0.12	-0.84	7.28	6.02	0.13	-2.42
	0.8	10.95	8.86	0.19	-1.90	12.56	16.53	0.14	-1.21
	1.1	23.54	5.45	0.18	-7.12	26.25	11.85	0.19	-3.14
QuattroJet	0.5	3.17	-0.69	0.10	-1.62	2.77	-0.26	0.10	-1.38
	0.8	7.16	-1.47	0.14	-4.02	11.00	-3.45	0.16	-7.08
	1.1	12.07	3.86	0.18	-4.30	101.52	-17.78	0.16	-96.50
MiniJet	0.5	35.67	4.74	0.05	-16.92	1.26	-4.25	4.37	-1.10
	0.8	34.25	13.55	0.15	-4.59	37.35	12.48	0.13	-6.99
	1.1	-	-	-	-	-	-	-	-

Measured droplet size distribution

The droplet size distributions were measured to evaluate how the volume of droplets is distributed across various size ranges under different flow rates and nebulizers. Fig. 6 (left panels) displays the

a supprimé: $(y = \frac{L}{1+e^{-k(x-x_0)}} + b)$

a supprimé: L

a supprimé: x

a supprimé: L

a supprimé: x

a mis en forme : Double souligné

a mis en forme : Double souligné

volume-weighted distribution density curves for droplets generated by different nebulizers, while Fig. 6 (right panels) shows the corresponding volume-weighted median diameters, D(v,0.5). The data presented represents the mean of three measurements, with error bars indicating standard deviations. Table 3 presents the volume weighted mean and median droplet size distribution for each nebulizer across multiple flow rates, ranging from 0.5 mL/s to 1.5 mL/s, where applicable.

The logarithm of the sizes distributions were fitted using a double Gaussian distribution function, which is commonly used for modeling bimodal distributions, peak detection, and spectral analysis (Squires, 2001):

$$Pr = c_1 . e^{-\frac{(log10(d)-log10(<d1>))^2}{2\sigma_1^2}} + c_2 . e^{-\frac{(xlog10(d)-log10(<d2>)^2}{2\sigma_2^2}} \quad (3)$$

where c_1 and c_2 represent the amplitudes (heights of the two peaks), μ_1 and μ_2 correspond to the means (positions of the peak centers), and σ_1 and σ_2 define the standard deviations (widths of the peaks).

This approach enables the extrapolation of bimodal size distribution curves. In Fig. 6, the black dashed lines represent the fitted curves overlaid on the original size distribution data. Table 4 presents the curve-fitting parameters for the extrapolated double Gaussian function, applied to the size distribution values at three different flow rates (0.5, 0.8, and 1.1 mL/s) across six nebulizers.

At a flow rate of 0.5 mL/s, the MCR-4 TOPOL and QuattroJet nebulizers failed to achieve stable aerosolization, likely due to incomplete development of the aerosolization process at this low flow rate. The remaining nebulizers produced stable aerosols, with the MiniJet generating the finest median droplet distribution (26.20 µm) and CapnoPharm exhibiting the coarsest (48.30 µm). For Capnopen, the median droplet size, D(v,0.5), was 30.5 µm. When the flow rate increased to 0.8 mL/s, all six nebulizers successfully generated aerosols. The MCR-4 TOPOL produced the largest droplets with the coarsest distribution (121 µm), followed by the QuattroJet (56.20 µm). In contrast, MiniJet, HurriChem, and CapnoPharm achieved the finest distributions.

At 1.1 mL/s, the MiniJet nebulizer faced structural limitations, causing disconnections between the high-pressure line and the nebulizer. Conducting the test was not feasible. The MCR-4 TOPOL and QuattroJet continued to produce coarser size distributions, while HurriChem and CapnoPharm demonstrated better performance with finer droplet distributions. In general, the results showed that increasing the flow rate reduced the mean droplet size across most nebulizers, highlighting the role of flow rate in producing finer aerosols. For Capnopharm and HurriChem nebulizers, increasing the flow rate from 0.8 to 1.1 mL/s did not result in any noticeable difference in the droplet size distribution.

At the highest flow rate of 1.5 mL/s, only the QuattroJet nebulizer was operational. Notably, increasing the flow rate from 1.1 to 1.5 mL/s did not result in any significant change in the droplet size distribution.

MCR-4 TOPOL is the most unimodal nozzle regarding the ratio C2/C1. On the other hand, this nozzle produces the largest droplets.

$$y = c_1 . e^{-\frac{(x-\mu_1)^2}{2\sigma_1^2}} + c_2 . e^{-\frac{(x-\mu_2)^2}{2\sigma_2^2}}$$

a supprimé: demonstrates

a supprimé: .

a déplacé (et inséré) [2]

a supprimé: data

a supprimé: y

a supprimé: x

a supprimé: $\mu 1$

a supprimé: $-\mu 2$

a supprimé: ¶

a déplacé vers le haut [2]: The size distribution data were fitted using a double Gaussian distribution function, which is commonly used for modeling bimodal distributions, peak detection, and spectral analysis (Squires, 2001):¶

$y = c_1 . e^{-\frac{(x-\mu_1)^2}{2\sigma_1^2}} + c_2 . e^{-\frac{(x-\mu_2)^2}{2\sigma_2^2}}$ →→(3)¶

¶

where c_1 and c_2 represent the amplitudes (heights of the two peaks), μ_1 and μ_2 correspond to the means (positions of the peak centers), and σ_1 and σ_2 define the standard deviations (widths of the peaks).¶

extrapolation of bimodal size distribution curves. In Fig. 6, the black dashed lines represent the fitted curves overlaid on the original size distribution data. Table 4 presents the curve-fitting parameters for the extrapolated double Gaussian function, applied to the size distribution values at three different flow rates (0.5, 0.8, and 1.1 mL/s) across six nebulizers.¶

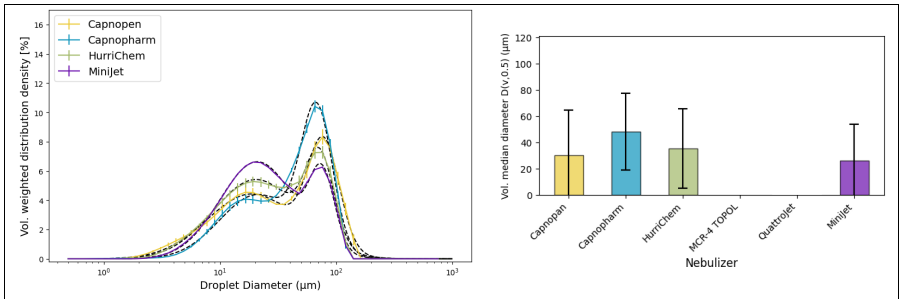

(a) flow rate= 0.5 mL/s

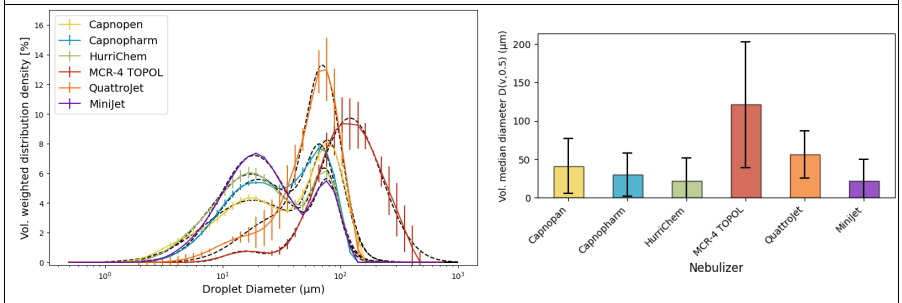

(c) flow rate= 0.8 mL/s

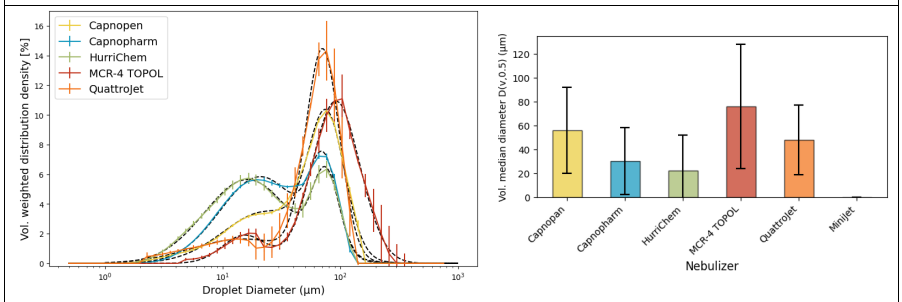

(c) flow rate= 1.1 mL/s

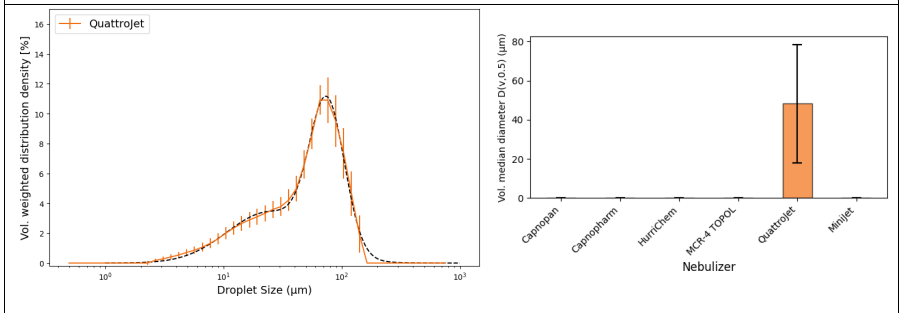

(d) flow rate= 1.5 mL/s

Fig. 6. DSD curves of nebulized saline (0.9% NaCl) showing the volume weighted distribution density (left curves) and volume weighted median diameter D(v,0.5) (right curves) for flow rate of (A) 0.5, (B) 0.8, (C) 1.1, and (D) 1.5 mL/s for six different nebulizers. Mean droplet diameters were measured (n = 3 for each confirmation) in a range of 0.5 to 900 µm. The error bars show one time the standard deviation. 20 mL of saline was nebulized in a close reconstructed peritoneal cavity for four different flow rates (0.5, 0.8, 1.1, and 1.5 mL/s) and a maximal upstream injection pressure of 21 bar. The black dashed lines represent the fitted curves overlaid on the original size distribution data.

Table 3. Mean and median droplet size distributions (D(v,0.5)) generated by six different nebulizers at varying flow rates. The table presents the average droplet size and median values for each nebulizer across multiple flow rates, ranging from 0.5 mL/s to 1.5 mL/s, where applicable.

Commenté [MOU6]: table 3 and table 4 can be merged

Nebulizer	Flow rate (mL/s)	Vol. weighted droplet size [µm]	
		Mean	Median
Capnopen	0.5	45.20	30.50
	0.8	45.74	41.40
	1.1	55.62	56.20
Capnopharm	0.5	46.20	48.30
	0.8	39.38	30.50
	1.1	38.49	30.50
HurriChem	0.5	39.66	35.60
	0.8	35.26	22.50
	1.1	35.06	22.50
MCR-4 TOPOL	0.8	140.79	121
	1.1	92.60	76.30
QuattroJet	0.8	61.19	56.20
	1.1	57.01	48.30
	1.5	56.64	48.30
MiniJet	0.5	36.48	26.20
	0.8	33.72	22.50

Table 4. Parameters of the extrapolated double Gaussian curve-fitting function, ($y = c_1.e^{(-\frac{(x-\mu_1)^2}{2\sigma_1^2})} + c_2.e^{(-\frac{(x-\mu_2)^2}{2\sigma_2^2})}$), applied to the size distribution data for three different flow rates (0.5, 0.8, and 1.1 mL/s) across six nebulizers.

Nebulizer		Parameters

	Flow rate (mL/s)	C_1	µ1	σ1	C2	µ2	σ2
Capnopen	0.5	4.43	18.81	0.38	7.12	78.28	0.13
	0.8	4.18	18.09	0.41	7.03	69.79	0.14
	1.1	3.48	23.66	0.37	9.00	76.70	0.15
Capnopharm	0.5	4.38	21.09	0.32	9.39	68.36	0.13
	0.8	5.58	20.22	0.33	6.35	69.37	0.13
	1.1	5.84	21.00	0.34	5.75	72.40	0.12
HurriChem	0.5	5.42	20.46	0.37	5.77	72.47	0.12
	0.8	5.94	17.48	0.35	5.13	75.55	2.01
	1.1	5.64	16.31	0.37	5.42	75.54	0.11
MCR-4 TOPOL	0.8	0.72	14.94	-0.15	9.71	120.96	0.27
	1.1	1.89	15.39	0.10	10.93	91.73	0.20
QuattroJet	0.8	3.04	30.38	0.31	11.79	71.88	0.15
	1.1	1.64	14.95 ?interesting ?	0.44	13.97	70.93	0.14
	1.5	3.42	24.54	0.36	9.78	75.34	0.15
MiniJet	0.5	6.63	20.98	0.32	4.95	75.91	0.11
	0.8	7.20	18.60	0.30	4.79	78.58	0.10

a mis en forme : Couleur de police : Texte 1, Surlignage

a mis en forme : Surlignage

a mis en forme : Surlignage

Effect of liquid flow rate on nebulization cone angle

The impact of liquid flow rate on the nebulization cone angle was thoroughly analyzed using high-resolution imaging and measurement techniques.

a déplacé vers le haut [3]: Fig. 7 provides a microscopic view of the orifices of the various nebulizers used in this study. High-speed camera imagery (Phantom) was employed to capture detailed photographs, ensuring precise measurements of the orifice diameters. Calibration of the scale was conducted using a known reference, enabling accurate pixel-to-distance conversion. The measured diameters of the nebulizer orifices were as follows: Capnopen: Ø ≈ 190 ± 2 µm; Capnopharm: Ø ≈ 186 ± 4 µm; HurriChem: Ø ≈ 191 ± 2 µm; MCR-4 TOPOL: Ø ≈ 389± 6 µm; QuattroJet : Ø ≈ 190 ± 2 µm; MiniJet: Ø≈160±2 µm. These measurements demonstrate significant variations in orifice sizes, which are expected to influence the spray characteristics.

Fig. 8 presents digital images illustrating the spray cone angle (Θ) and the formation of the spray pattern in a 2D plane for each nebulizer. The experiments were conducted using saline solution (0.9% NaCl), with two flow rates: 0.8 mL/s and 1.1 mL/s. For the MiniJet, however, the flow rates used were 0.5 mL/s and 0.8 mL/s. The spray cone angle was measured for each nebulizer to assess the influence of flow rate on nebulization performance. The results indicate a trend where an increase in the flow rate results in a little wider spray cone angle. This effect can be attributed to the higher momentum of the liquid exiting the nozzle, which leads to better dispersion of the aerosolized droplets and enhances the spray process.

The MCR-4 TOPOL nebulizer produced the largest spray cone angle among all tested devices, which can be linked to its larger orifice diameter and different design. The larger orifice allows for higher liquid throughput, thereby producing a broader cone angle.

At the lower flow rate of 0.8 mL/s, both the MCR-4 TOPOL and QuattroJet nebulizers did not exhibit a uniform spray pattern, likely due to insufficient pressure buildup needed to generate a stable aerosol. However, at higher flow rates (>1.0 mL/s), these nebulizers achieved a uniform spray, highlighting the importance of sufficient flow rate for consistent nebulization.

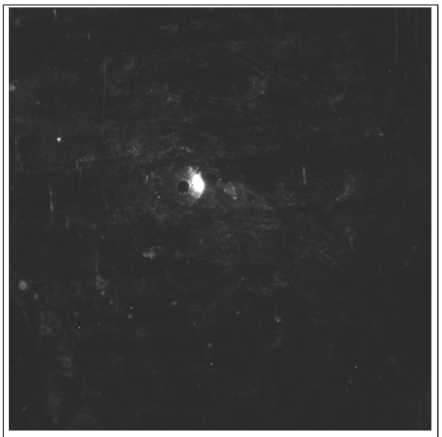

(a) Capnopen: Ø≈190±2 µm

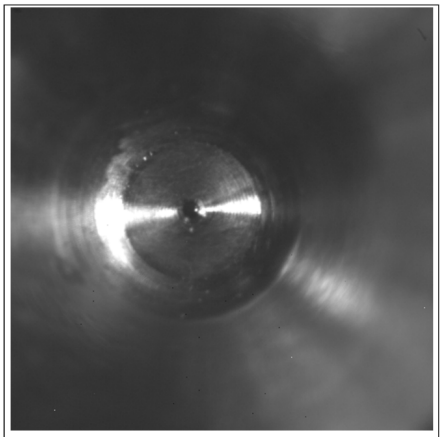

(b) Capnopharm: Ø≈186±4 µm

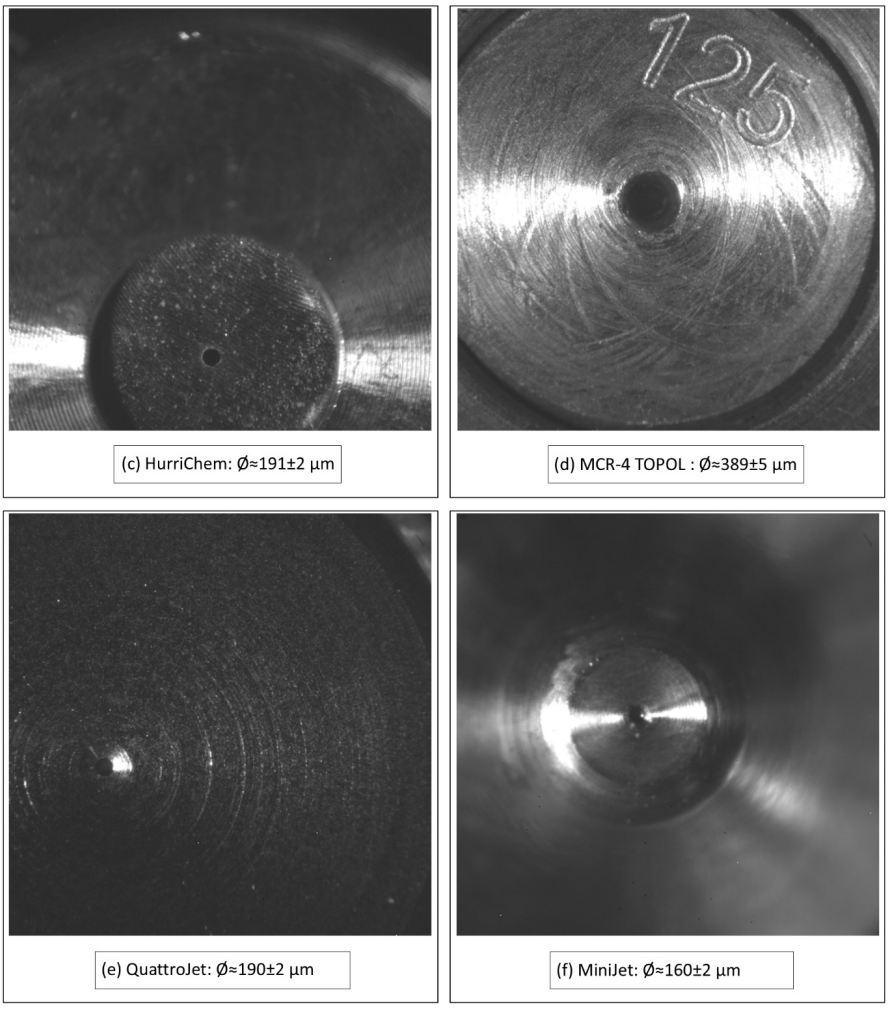

Fig. 7. Microscopic visualization of the orifices of nebulizers.

Flow rate= 0.8 mL/s

Flow rate= 1.1 mL/s

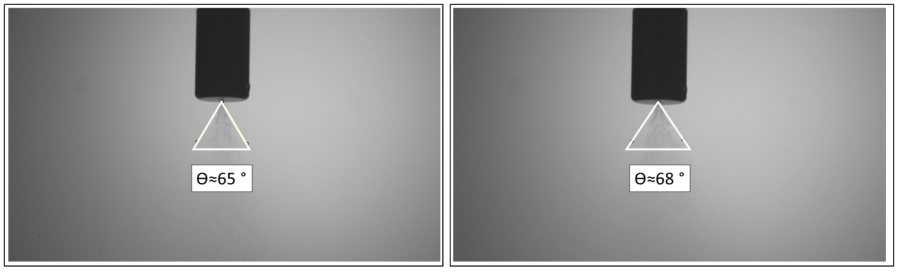

(a) Capnopen

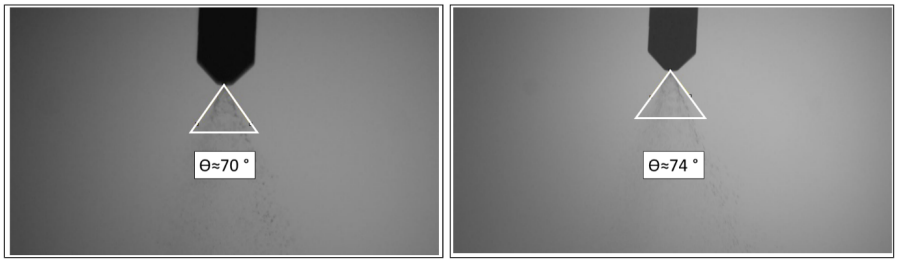

(b) Capnopharm

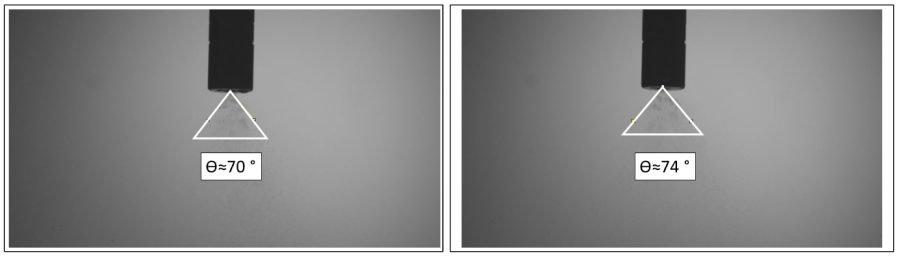

(c) HurriChem

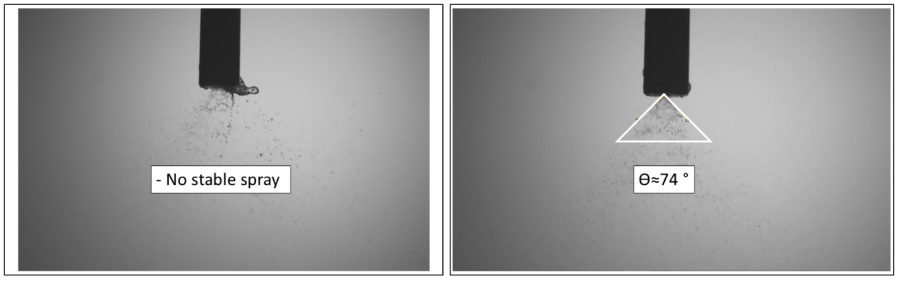

(d) MCR-4 TOPOL

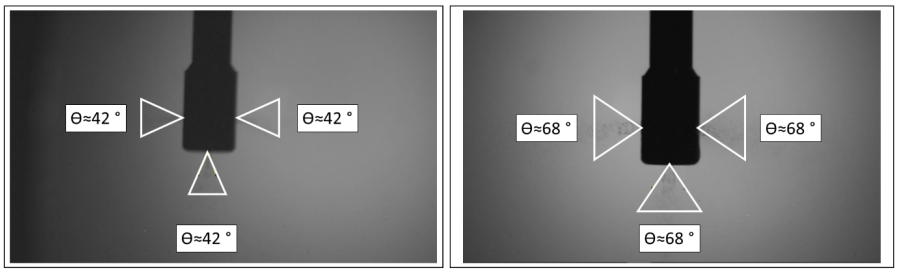

(e) QuattroJet

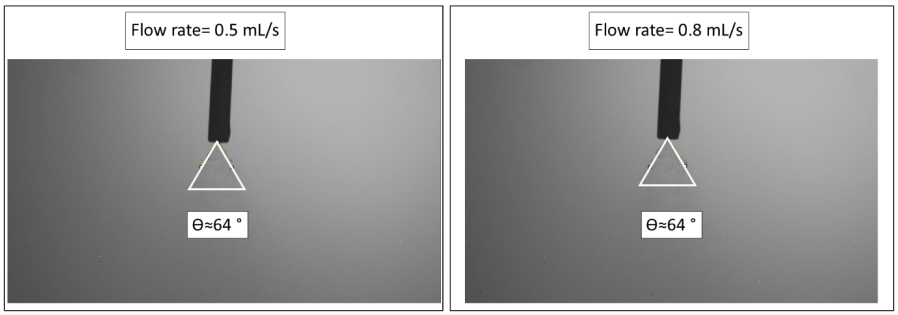

(f) MiniJet

Fig. 8. Visual representation of nebulized saline (0.9% NaCl) for all nebulizers at two flow rates (0.8 and 1.1 mL/s- For MiniJet, 0.5 and 0.8 mL/s were used), with the spray cone angle (Θ) illustrated for each case.

Discussion

Due to the very less known of investigation of the operating characteristics of nebulizers used for intraperitoneal aerosolized drug delivery, six nebulizers were comparatively analysed. The most important determined technical characteristics of these nebulizers were operational pressure, droplet size distribution, and spray cone angle.

Observing each nebulizer's performance, it's clear that the operational pressure increases proportionally with the flow rate, a pattern consistent across all devices. This correlation suggests that higher flow rates necessitate greater pressure to maintain consistent nebulization, which directly impacts the nebulization efficiency and characteristics.

In many cases, the operational pressure was observed to taper off, aligning with expected outcomes due to resistance within the system. However, deviations from this pattern were noted, particularly for the MCR-4 Topol. These discrepancies could be attributed to partial obstructions within the nebulizer or unique elements of its design that impact fluid dynamics. This is also certainly due to the size of the aperture. Furthermore, the practical pressures observed in the high-pressure line were lower than the

Commenté [MOU7]: I would say that the diameter is much larger than the other ones, no ?

pressures recorded at the high-pressure pump. This discrepancy can be explained by the pressure loss that occurs as the liquid travels through the system. The main contributors to this pressure drop can be dimensional mismatch includes a 50 mm diameter syringe connected to a 2 mm diameter high-pressure tube, creating a significant bottleneck that results in pressure loss. The 200 cm length of the high-pressure tube introduces additional resistance, with longer distances exacerbating pressure loss. Given this setup, higher flow rates require the high-pressure pump to exert even greater pressure to overcome these resistances and maintain efficient nebulization.

The findings underscore the importance of selecting an appropriate nebulizer based on the specific requirements of the application. For high flow rates exceeding 1 mL/s, the Quattrojet proves optimal, achieving maximum pressure slowly, which is advantageous for applications that demand a higher flow rate. However, for scenarios where lower pressure is adequate or desired, Capnopharm and HurriChem are viable alternatives, offering steady pressure without the sharp rise seen in the Capnopen.

A bimodal volume-weighted DSD was consistently observed across nebulizers when saline (0.9% NaCl) was nebulized in a closed, reconstructed peritoneal cavity. The bimodal pattern is attributed to the presence of two distinct length scales of liquid ligaments during atomization (Chen & Ashgriz, 2022). Fine droplets arise from the breakup of thinner liquid threads, remaining suspended in the aerosol for extended periods, while larger droplets settle more rapidly due to gravitational effects. This size disparity could be influenced by secondary flow phenomena, such as turbulence, as well as the specific aerosolization mechanisms of each nebulizer.

Overall, the MCR-4 TOPOL consistently generated the largest droplets, indicating limited spatial distribution capability, whereas the MiniJet and HurriChem produced finer aerosols, particularly at moderate flow rates (0.8 mL/s), leading to superior spatial distribution. The bimodal distribution patterns observed across nebulizers emphasize the significance of fine droplets, typically between 10 and 20 µm, in achieving homogeneous aerosol distribution. These fine droplets are less influenced by gravity, enhancing deposition uniformity. Additionally, smaller droplet sizes correlate with an increased cone angle, which improves the spatial coverage of the aerosol (Braet et al., 2021). Consequently, nebulizers such as HurriChem are better suited for applications requiring precise and uniform aerosol distribution, while the MCR-4 TOPOL and QuattroJet may be more appropriate for applications where larger droplet sizes are needed. These findings highlight the importance of selecting nebulizers based on their droplet size distribution characteristics, spatial aerosol distribution, and operating flow rate capabilities.

The Capnopharm and HurriChem nebulizers showed robust performance, generating a stable spray with relatively large cone angles even at the lower flow rate. This suggests that their design and optimized orifice sizes are more effective at aerosolizing liquid at varying flow rates. The uniform spray pattern at both flow rates for these devices indicates better adaptability to varying operating conditions, making them suitable for applications requiring precise control over aerosol dispersion.

The difference in spray cone angles and uniformity of nebulization between the devices can be attributed to the mechanical structure, design of the nozzle, and the orifice size. Larger orifices, like in the MCR-4 TOPOL, facilitate higher flow rates, which in turn can create broader cone angles but require higher pressure to achieve uniform spray patterns, and they produce significantly larger droplets compared to other nebulizers.

Smaller orifices, as seen in all nebulizers except MCR-4 TOPOL, allow for efficient atomization even at lower flow rates due to better fluid control and optimized nozzle design, resulting in stable and consistent aerosol formation.

The MiniJet nebulizer struggled to operate effectively at flow rates exceeding 0.5 mL/s due to its design and structure, which are optimized for low flow rates. No significant difference was observed in the cone angle between flow rates of 0.5 mL/s and 0.8 mL/s. However, at a flow rate of 0.8 mL/s, the connection between the high-pressure line and the nebulizer frequently disconnected after some time. This indicates that the nebulizer is not suitable for high flow rates.

The extent to which nebulizer's design and its spray characteristics affect the spatial distribution, penetration depth and tissue concentration of drugs has hardly been investigated so far.

The QuattroJet's innovative four-nozzle design was developed to enhance spatial drug distribution in the peritoneal cavity. However, Sautkin et al. (Sautkin, Weinreich, & Reymond, 2024) reported that the increased number of spray nozzles in a multi-nozzle nebulizer did not fulfill its intended goals. They observed that this design did not improve tissue drug delivery, or the homogeneity of tissue drug distribution as initially anticipated. In contrast, a recent study by Braet et al. (Braet et al., 2023) examined the administration of nanoparticles in an ex-vivo model using a Capnopen and a multidirectional nebulizer (Medspray). Their findings indicated that the multidirectional nozzle achieved a more homogeneous spatial distribution pattern of the nanoparticles compared to the Capnopen, highlighting the potential advantages of multidirectional spray technology for uniform aerosol delivery.

Further supporting this notion, Goehler et al. (Göhler, Große, et al., 2017) investigated the performance of the Capnopen and a two-substance nozzle in a pig model. They demonstrated that the two-substance nozzle produced finer droplet sizes, resulting in significantly more homogeneous spatial distribution of ^{99m}Tc pertechnetate and improved penetration depth of doxorubicin.

The chemical resistance or composition of the nebulizers was not examined in this study. However, Goehler et al. (Göhler et al., 2024) provided an insightful visualization of the nebulizer components following exposure to cytostatic solutions. Their findings revealed that, in the case of the MCR-4 TOPOL nebulizer, such exposure resulted in the formation of iron oxide on its surfaces.

Conclusions

Intraperitoneal aerosolized drug delivery holds considerable promise for the treatment of peritoneal cancer. This study provides a comprehensive evaluation of six nebulizers— Capnopen (REGER 770-12), Capnopharm, HurriChem, MCR-4 TOPOL (Skala), QuattroJet (REGER 770-14), and MiniJet (REGER 770-15)—examining critical performance parameters such as operational pressure, droplet size distribution, and spray cone angle. These findings offer significant insights into the physiological and technical aspects of IPADD.

The study highlights key distinctions in nebulizer performance. Devices like MiniJet and HurriChem produced the finest droplets, while QuattroJet's unique four-nozzle design demonstrated superior spatial drug distribution potential. Increased flow rates enhanced aerosol pressure and dispersion, potentially improving treatment efficacy, while spray cone angles emphasized the need for sufficient flow to achieve uniform nebulization. Additionally, understanding device-specific pressure dynamics, such as the unique performance of the MCR-4 TOPOL, is crucial for optimizing treatment outcomes.

The findings highlight the complexities of designing nebulizers for IPADD, emphasizing that efficacy relies on precise engineering tailored to specific therapeutic requirements. However, the clinical impact on oncologic outcomes remains uncertain, necessitating extensive preclinical and clinical research. Future studies should explore how physiological factors—such as humidity, temperature, and pH—interact with pressure profiles and droplet dynamics to enhance tissue penetration and drug

distribution. Notably, no CO_2 was introduced into the model. However, future investigations should consider the potential impact of continuous CO_2 flow on droplet size distribution.

By building on these insights, healthcare professionals can tailor nebulizer selection and treatment protocols to individual patient needs, potentially enhancing therapeutic precision, drug delivery efficacy, and clinical outcomes. Advancements in IPADD technology and methodology could significantly improve the prognosis and quality of life for patients with peritoneal cancer, paving the way for more effective, personalized interventions.

Competing interests: The authors declare no competing interests.

Ethics statement:

Acknowledgements: This work was supported by the Research Foundation - Flanders (FWO, Brussels, Belgium) under Grant 1249925N to Mohammad Rahimi-Gorji. Wim Ceelen is a senior clinical investigator from the FWO. The authors thank Valerie Vanhoorne (Laboratory of Pharmaceutical Technology, Faculty of Pharmaceutical Sciences, Ghent University) for her assistance with laser diffraction studies, and Jurgen Deviche (Techinical staff, BioMMeddA) for his support with the calibration procedure and data collection. The authors also acknowledge the support of REGER Medizintechnik (Villingendorf, Germany), CapnoPharm (Tubingen, Germany), ThermaSolutions (White Bear Lake, MN, USA), and SKALA-Medica (Soběslav, Czech Republic) for providing the nebulizers. Stéphane Dorbolo is a F.R.S.-FNRS Senior Research Associate.

REFERENCES

Alyami, M., Hübner, M., Grass, F., Bakrin, N., Villeneuve, L., Laplace, N., . . . Kepenekian, V. (2019). Pressurised intraperitoneal aerosol chemotherapy: rationale, evidence, and potential indications. *The Lancet Oncology, 20*(7), e368-e377.

Braet, H., Andretto, V., Mariën, R., Yücesan, B., van der Vegte, S., Haegebaert, R., . . . Remaut, K. (2023). The effect of electrostatic high pressure nebulization on the stability, activity and ex vivo distribution of ionic self-assembled nanomedicines. *Acta Biomaterialia, 170*, 318-329.

Braet, H., Rahimi-Gorji, M., Debbaut, C., Ghorbaniasl, G., Van Walleghem, T., Cornelis, S., . . . Ceelen, W. (2021). Exploring high pressure nebulization of Pluronic F127 hydrogels for intraperitoneal drug delivery. *European Journal of Pharmaceutics and Biopharmaceutics, 169*, 134-143.

Ceelen, W., Braet, H., Van Ramshorst, G., Willaert, W., & Remaut, K. (2020). Intraperitoneal chemotherapy for peritoneal metastases: an expert opinion. *Expert opinion on drug delivery, 17*(4), 511-522.

Chen, S., & Ashgriz, N. (2022). Droplet size distribution in swirl nozzles. *International Journal of Multiphase Flow, 156*, 104219.

Göhler, D., Große, S., Bellendorf, A., Falkenstein, T. A., Ouaissi, M., Zieren, J., . . . Giger-Pabst, U. (2017). Hyperthermic intracavitary nanoaerosol therapy (HINAT) as an improved approach for pressurised intraperitoneal aerosol chemotherapy (PIPAC): Technical description, experimental validation and first proof of concept. *Beilstein Journal of Nanotechnology, 8*(1), 2729-2740.

Göhler, D., Khosrawipour, V., Khosrawipour, T., Diaz-Carballo, D., Falkenstein, T. A., Zieren, J., . . . Giger-Pabst, U. (2017). Technical description of the microinjection pump (MIP®) and granulometric characterization of the aerosol applied for pressurized intraperitoneal aerosol chemotherapy (PIPAC). *Surgical endoscopy, 31*, 1778-1784.

Göhler, D., Oelschlägel, K., Ouaissi, M., & Giger-Pabst, U. (2024). Performance of different nebulizers in clinical use for Pressurized Intraperitoneal Aerosol Chemotherapy (PIPAC). *Plos one, 19*(5), e0300241.

Khosrawipour, V., Khosrawipour, T., Diaz-Carballo, D., Förster, E., Zieren, J., & Giger-Pabst, U. (2016). Exploring the spatial drug distribution pattern of pressurized intraperitoneal aerosol chemotherapy (PIPAC). *Annals of surgical oncology, 23*, 1220-1224.

Kobayashi, D., & Kodera, Y. (2017). Intraperitoneal chemotherapy for gastric cancer with peritoneal metastasis. *Gastric Cancer, 20*(Suppl 1), 111-121.

Meyers, R. A. (1992). Encyclopedia of physical sciences and technology. *San Diego: Academic Press*.

Nadiradze, G., Horvath, P., Sautkin, Y., Archid, R., Weinreich, F.-J., Königsrainer, A., & Reymond, M. A. (2019). Overcoming drug resistance by taking advantage of physical principles: pressurized intraperitoneal aerosol chemotherapy (PIPAC). *Cancers, 12*(1), 34.

Parmentier, J., Terrapon, V., & Gilet, T. (2023). Drop impact on thin film: Mixing, thickness variations, and ejections. *Physical Review Fluids* 8, 053603.

Rahimi-Gorji, M., Debbaut, C., Ghorbaniasl, G., Cosyns, S., Willaert, W., & Ceelen, W. (2022). Optimization of intraperitoneal aerosolized drug delivery using computational fluid dynamics (CFD) modeling. *Scientific Reports, 12*(1), 6305.

Rahimi-Gorji, M., Ghorbaniasl, G., Cosyns, S., Willaert, W., & Ceelen, W. (2021). *Effect of fluid flow rate and droplet size on spatial aerosol distribution during pressurized intraperiational aerosol chemotherapy (PIPAC).* Paper presented at the 26th Congress of the European Society of Biomechanics (ESB 2021): European Society of Biomechanics.

Rahimi-Gorji, M., Van de Sande, L., Debbaut, C., Ghorbaniasl, G., Braet, H., Cosyns, S., . . . Ceelen, W. (2020). Intraperitoneal aerosolized drug delivery: technology, recent developments, and future outlook. *Advanced Drug Delivery Reviews, 160*, 105-114.

Rioboo, R., Tropea, C., & Marengo, M. (2001). Outomes from a drop impact on solid surfaces, *Atomization and Sprays* 11, 155

Sautkin, Y., Weinreich, J., & Reymond, M. A. (2024). A multi-nozzle nebuliser does not improve tissue drug delivery during PIPAC. *Surgical Endoscopy, 38*(10), 5832-5841.

Sgarbura, O., Villeneuve, L., Alyami, M., Bakrin, N., Torrent, J. J., Eveno, C., . . . Mortensen, M. B. (2021). Current practice of pressurized intraperitoneal aerosol chemotherapy (PIPAC): Still standardized or on the verge of diversification? *European Journal of Surgical Oncology, 47*(1), 149-156.

Squires, G. L. (2001). *Practical physics*: Cambridge university press.

Stein, S. W., & Thiel, C. G. (2017). The history of therapeutic aerosols: a chronological review. *Journal of aerosol medicine and pulmonary drug delivery, 30*(1), 20-41.

a mis en forme : Police :Non Gras

a mis en forme : Espace Après : 0 pt

a supprimé: ¶

a mis en forme : Police :Italique

a mis en forme : Police :Italique